Electronic Supplementary Material (ESI) for Nanoscale.
This journal is © The Royal Society of Chemistry 2023

Supplementary Information

Metal-organic Frameworks-based Self-healing Hydrogel Fiber Random Lasers

Dexiang Zhu[a], Zhouyuanhang Wang[a], Jun Xie[a], Guangyin Qu[a], Qi Yu[a], Yan Kuai[a], Benli Yu[a], Jianzhong Zheng[b], Zhijia Hu[*a], Siqi Li[*a]

a.Information Materials and Intelligent Sensing Laboratory of Anhui Province, Key Laboratory of Opto-Electronic Information Acquisition and Manipulation of Ministry of Education, School of Physics and Optoelectronic Engineering, Anhui University, Hefei, 230601, Anhui, P. R. China

b. School of Environmental Science and Engineering, Nanjing Tech University, Nanjing, 211816, China

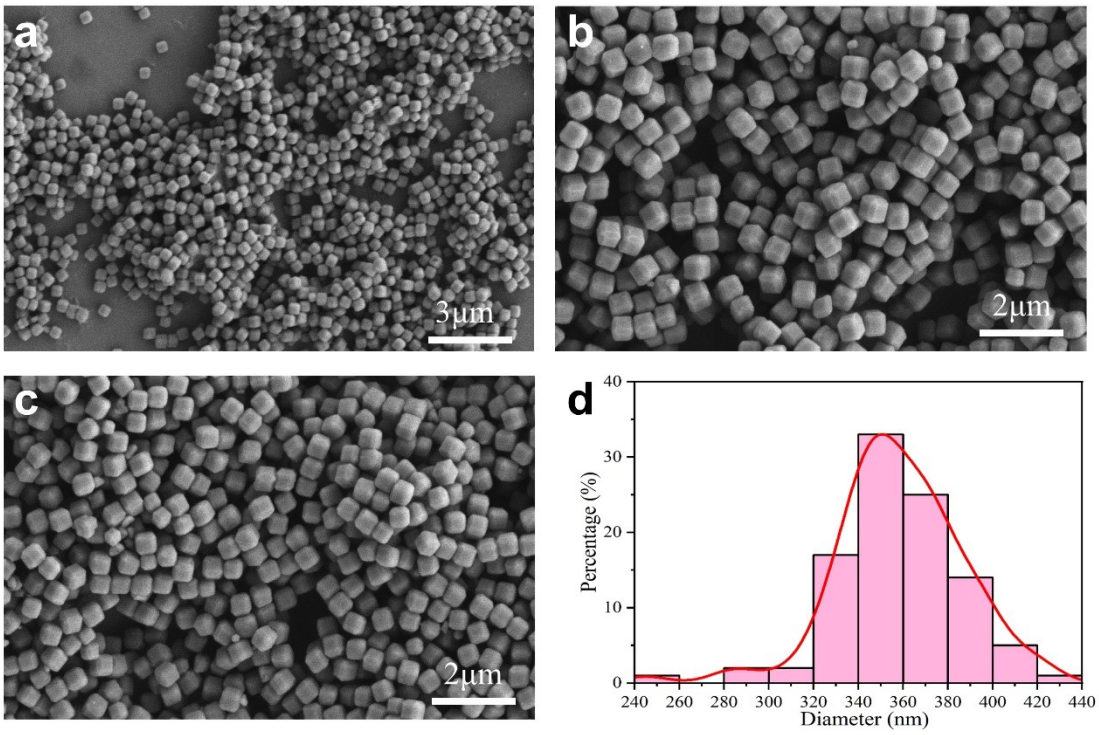

Figure S1. (a-c) SEM images of ZIF-8 nanoparticles. (d) Particle size distribution of ZIF-8 nanoparticles.

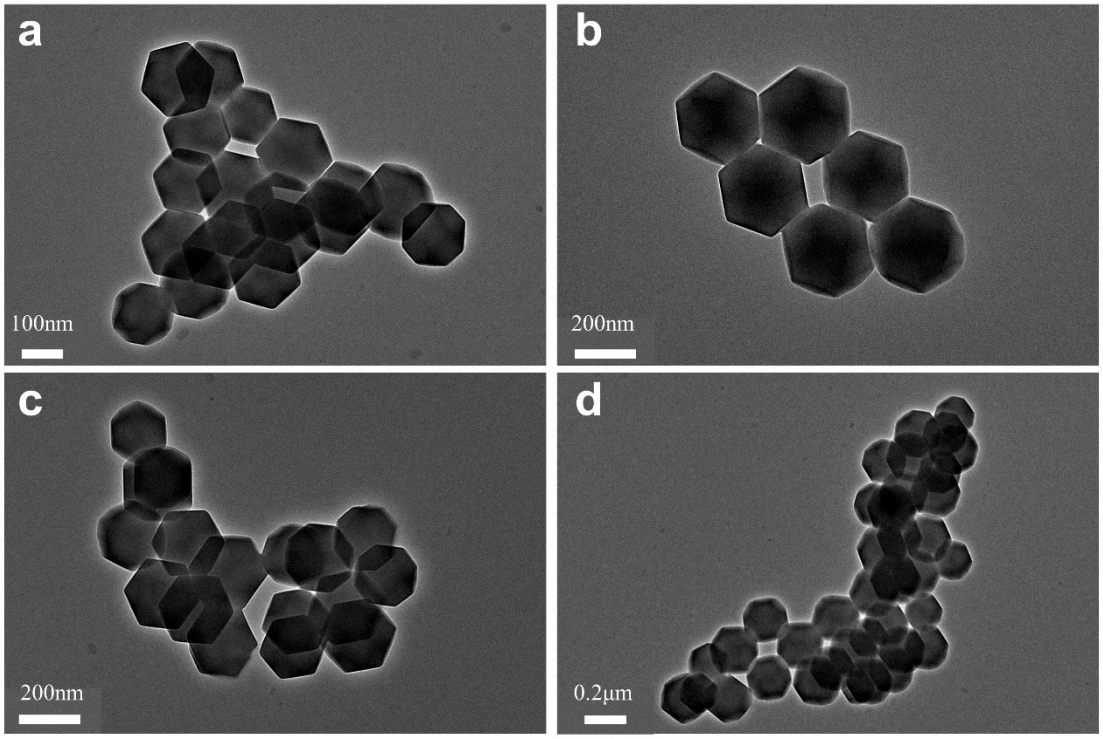

Figure S2. TEM images of ZIF-8 nanoparticles.

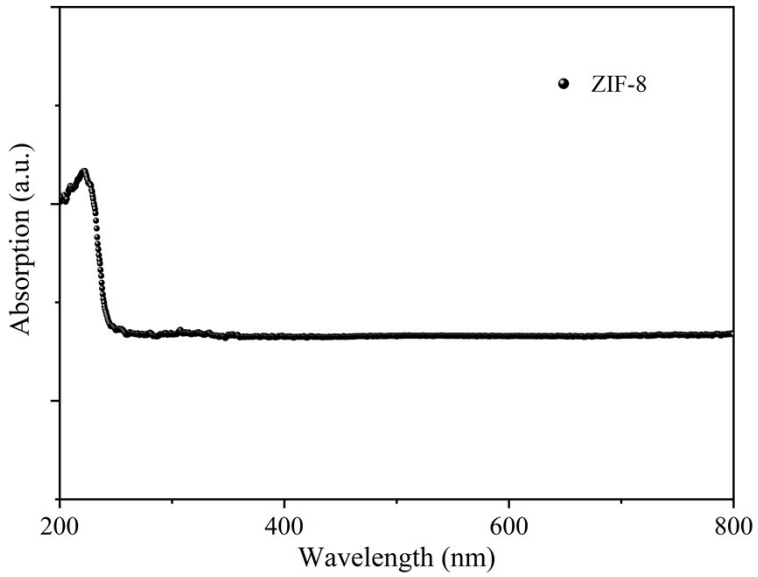

Figure S3. The absorption spectrum of ZIF-8.

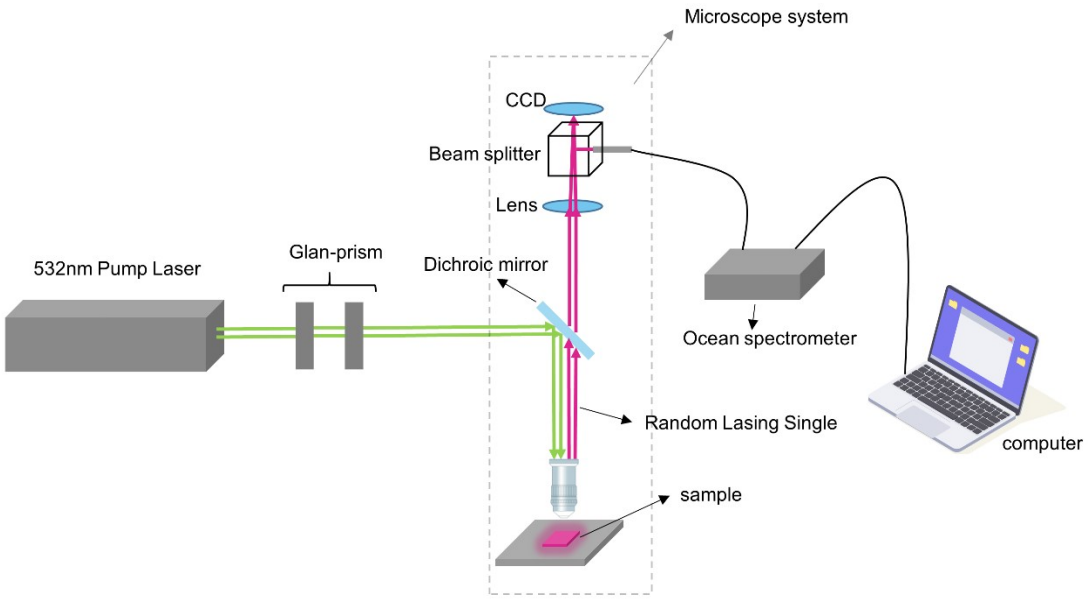

Figure S4. Test optical paths of microscope systems. The lasing beam of the pump light source (Q-Switched Nd: YAG lasers) goes through a Glan prism group consisting of two Glan prisms to control pulse polarization value and energy. The dichroic mirror reflects the pump lasing entering the microscope system and focuses on the sample. The lasing signal generated from the sample is collected by the microscope objective and focused onto the beam splitter through the focusing lens. The signals collected by the microscope system are partly sent to the CCD camera for imaging and partly collected by the fiber optic spectrometer (QE65PRO, Ocean Optics, resolution of ~0.4 nm, integration time of 100 ms) and sent to the computer for data processing.

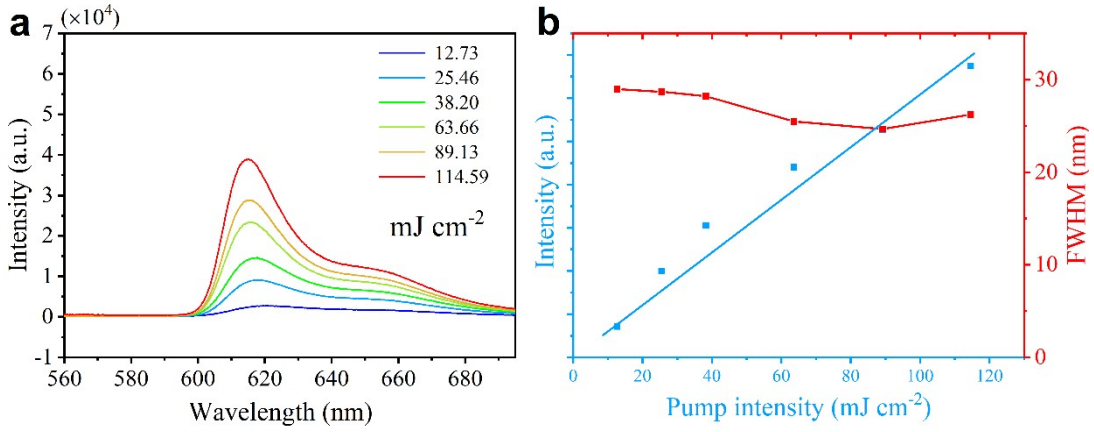

Figure S5. (a) Emission spectra of 0.7 wt% ZIF-8 doping at a dye concentration of 0.2 wt% (b) The variation of integrated emission intensity and FWHM with pump energy density.

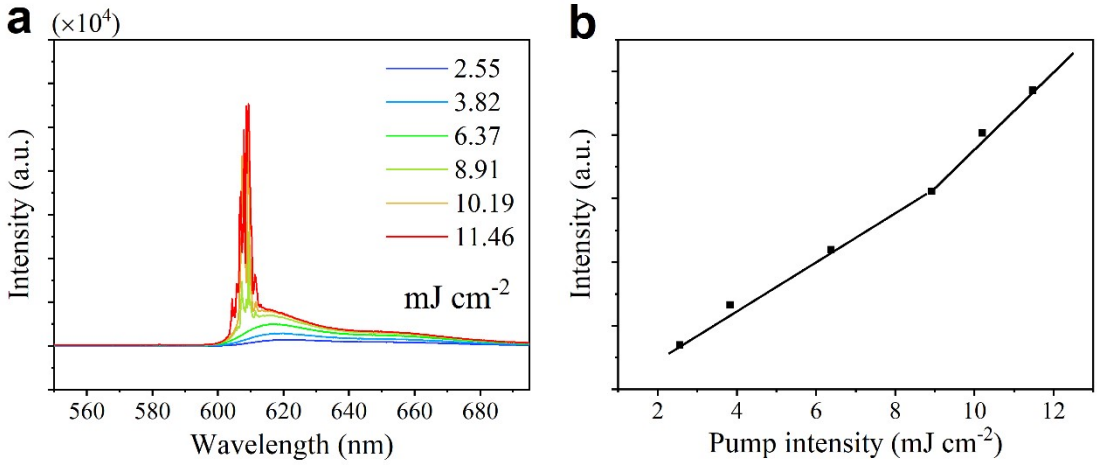

Figure S6. (a)Emission spectra of 0.7 wt% ZIF-8 doping at a dye concentration of 0.07 wt%. (b) The variation of integrated emission intensity with pump energy density.

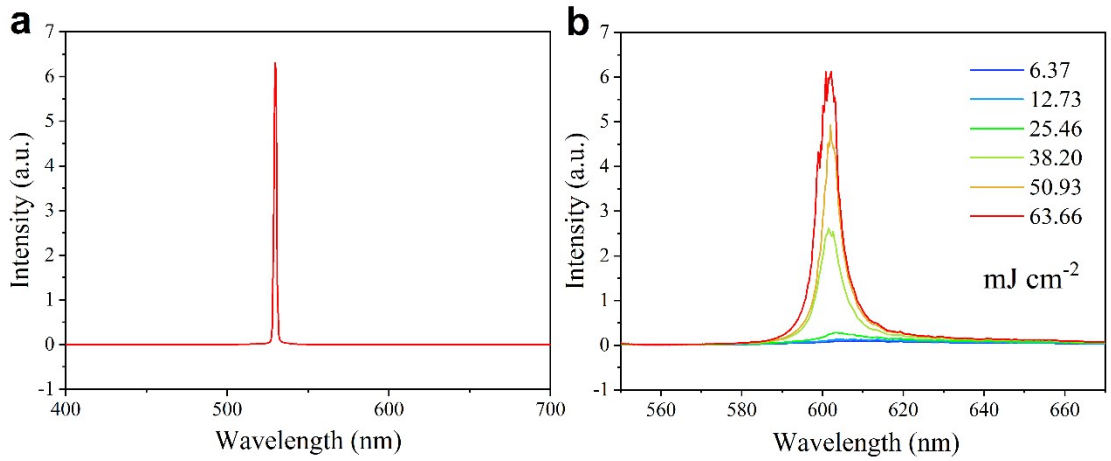

Figure S7. Spectra of the laser at the input (a) and output (b) of SHFRL.

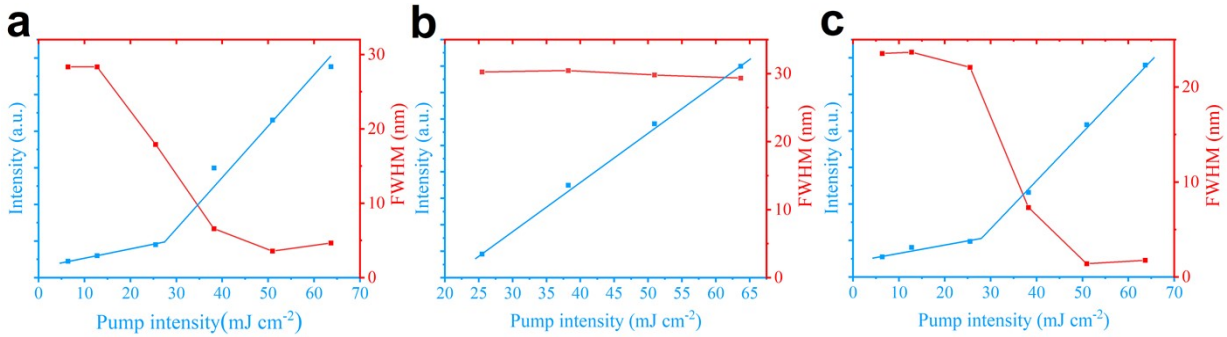

Figure S8. The variation of integrated intensity and FWHM with pump energy density of MOF-SHFRL (a) before fracture (b) after fracture (c) after self-healing.

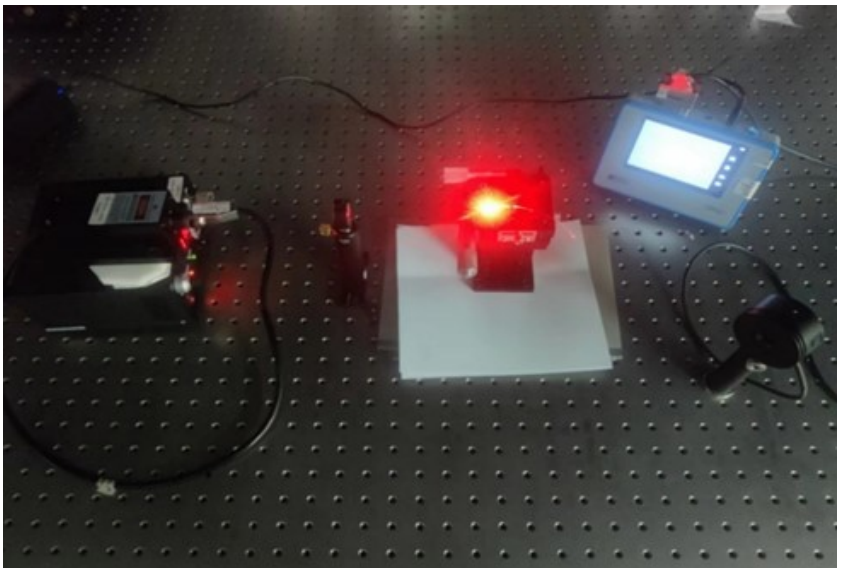

Figure S9. The photo of the optical path for MOF-SHFRL fracture loss test.